Comparison of F17 and F18 Daily Polar Gridded SSMIS Data

S. Stewart, H. Wilcox, W. Meier, D. Scott
August 2019

National Snow and Ice Data Center (NSIDC)

Introduction

The National Snow and Ice Data Center (NSIDC) archives and distributes polar gridded brightness temperature data sets derived from passive microwave satellite data, spanning more than 30 years. Currently, NSIDC produces the DMSP SSMI-SSMIS Daily Polar Gridded Brightness Temperatures (nsidc-0001) data set using data from the Defense Meteorological Satellite Programs Special Sensor Microwave/Imager and Special Sensor Microwave/Imager and Sounder (DMSP SSM/I-SSMIS). The data set is created using raw brightness temperatures processed by Remote Sensing Systems, Inc. (RSS). Because RSS performs various calibration and geolocation checks on the initial raw satellite data, there is a time lag of one to three month after the date of acquisition before NSIDC receives the brightness temperatures from RSS and data are distributed to users. The standard data set data are available for dates beginning 9 July 1987. Processing is ongoing.

This document summarizes and characterizes changes users should expect in nsidc-0001 DMSP SSMI-SSMIS Daily Polar Gridded Brightness Temperatures data set as a result of the transition from F17 SSMIS to F18 SSMIS as the source of the input data.

Overview of Processing F17 and F18 data

Brightness temperatures as observed by sensors aboard the Defense Meteorological Satellite Program (DMSP) are provided by RSS as swath files. The characteristics and processing of these data are described in the User Guide for this dataset, available at:

https://nsidc.org/data/nsidc-0001.

For the SSMIS sensors aboard F17 and F18, five lower frequency bands are detected at 25km (nominal) resolution: 19H, 19V, 22V, 37H, 37V. Two higher frequency bands are detected at 12.5km (nominal) resolution: 91H, 91V. The swath files consist of arrays of observations whose ground trace are a series of arcs. In addition, the latitude, longitude and detailed observational parameters about each observation are recorded for each point in the swath.

For the nsidc-0001 data set, these swath files are processed at the NSIDC DAAC to estimate brightness temperatures on the polar stereo grid with resolutions corresponding to those of the original swath data. If any data quality flags are raised for a data point, it is excluded and not used in the gridded data set. Brightness temperatures are gridded to polar stereographic grids using a daily drop-in-the-bucket average. If no valid data occur for a grid cell during a given day, the brightness temperature value is assigned a value of zero.

The F17 data is provided to the NSIDC DAAC as swath data in binary format, whereas the F18 swath data are provided in netCDF format. While the F17 data are RSS v07r01 and the F18 data are RSS v08r01, the only differences between the F17 and F18 fields are values that change with each swath, e.g. temporal and geolocation limits, as well as descriptions of the satellite (F17 vs F18). The same sensor information and geophysical data are provided for both satellites.

With the change of satellite from F17 to F18, we expect the following differences in the gridded brightness temperature values as a result of differences in the observed values:

- The satellites have different orbits, so the details of where observations are taken will be different between the two sensors.
- Because both F17 and F18 have SSMIS sensors, only minor differences between the F17 and F18 platforms are expected if the satellites observed the same scene.
- Data outage periods between the satellites are expected to by uncorrelated
- The crossing times of the satellites are similar, by design. This should have only a small effect on differences between F17 and F18 Tbs.
  - During the comparison year – 2015 – the F17 ascending node crossing time was ~18:20
  - During the comparison year – 2015 – the F18 ascending node crossing time was ~19:30
  - See http://www.remss.com/support/crossing-times/ for current status.
- Some channels are more affected by water vapor than others, and so higher differences are expected between the 22V and 91 GHz fields.

Comparison Methodology

In order to characterize the differences users are likely to expect with the nsidc-0001 data derived from F18, data from both sensors were compared during an overlap year 2015.

There were 16 days in 2015 for which at least one swath was missing for either F17 or F18, so these dates were excluded from the analysis: 1/22, 3/3, 3/14, 3/15, 5/3, 6/22, 6/20, 7/1, 7/26, 8/23, 8/24, 9/2, 9/15, 10/8, 10/27, 12/7.

On each day, statistics are computed on every pixel where both F17 and F18 have data. A linear regression results in a bias, slope and intercept, and a correlation coefficient is also computed. In addition, the standard deviation, and the number of pixels with particularly large differences (>10°K, >20°K, >50°K) are tabulated.

Brightness temperatures are tabulated separately for the Northern and Southern Hemispheres.

Because different users of the data set may concentrate on different locations, four masks – illustrated in Figure 1 – were developed to limit the comparisons:

- Water-only: Only grid cells at least 3 pixels away from land
- Land-only: Only grid cells at least 3 pixels away from water
- Seaice-all: Ocean pixels on where sea ice occurs, based on a climatology based on NSIDC 0051
- Seaice-noncoast: As per Seaice-all, except grid cells within 3 pixels of land are excluded.

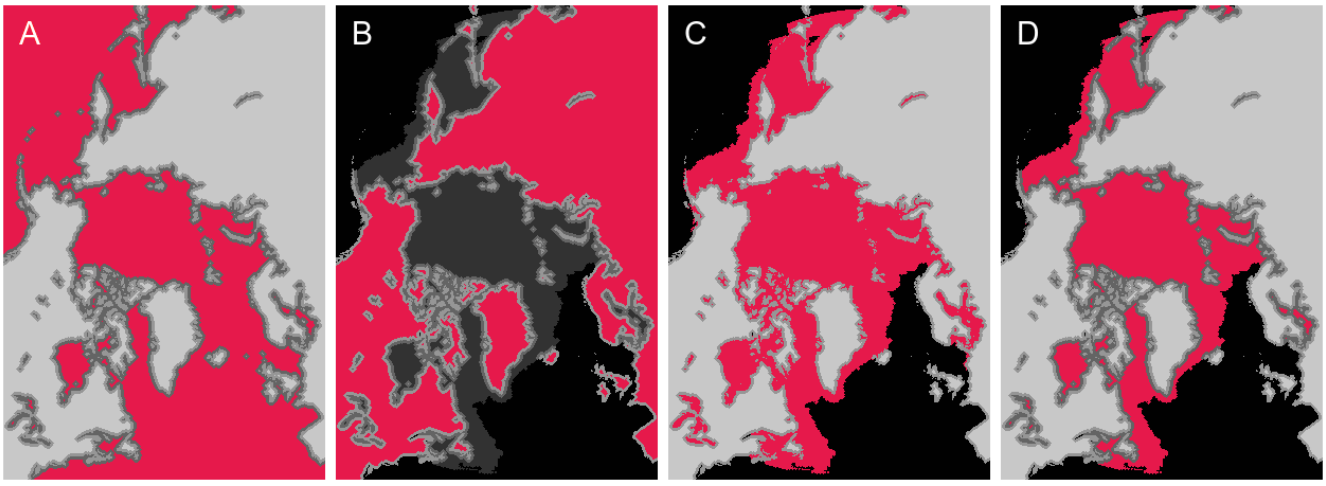

Figure 1: Masks used to limit the Tb comparisons. The red area shows which pixels were included in the comparisons. Different gray levels indicate land-far-from-water (lightest gray), land-near-water (slightly dark gray), water-near-land (dark gray), water-within-the-climatological-sea-ice (very dark gray), and water outside the climatological sea ice region (black). (A) shows the "water-only" mask region, (B) is "land-only", (C) is "sea ice", (D) is "sea ice except near land."

A summary of the results is tabulated in Tables 1 and 2. The means and standard deviations of each of the characteristics is computed for both hemispheres, all five channels, all-points and four mask types.

		Bias		Slope		Intercept		Correlation		Std Dev		Num > 10K		Num > 20K		Num > 50K	
Chan	Mask	Mean	(StdDev)	Mean	(StdDev)	Mean	(StdDev)	Mean	(StdDev)	Mean	(StdDev)	Mean	(StdDv)	Mean	(StdDv)	Mean	(StdDv)
n19h	all	0.6240	(0.2365)	1.0100	(0.0033)	-1.3389	(0.6457)	0.9963	(0.0011)	5.0776	(0.7230)	6641	(1501)	1558	(557)	87	(87)
n19h	water	-0.1391	(0.3018)	0.9983	(0.0113)	0.0786	(1.5091)	0.9882	(0.0081)	5.8917	(1.2153)	3324	(999)	972	(466)	80	(84)
n19h	land	1.3914	(0.4251)	1.0100	(0.0052)	-1.0749	(1.2082)	0.9946	(0.0019)	2.2630	(0.5045)	335	(308)	17	(28)	0	(1)
n19h	seaice	0.2226	(0.3106)	1.0080	(0.0041)	-1.2380	(0.6867)	0.9963	(0.0014)	4.0884	(0.4976)	1013	(310)	167	(89)	3	(7)
n19h	si-exc	0.1794	(0.3046)	1.0103	(0.0035)	-1.6768	(0.6511)	0.9986	(0.0007)	2.7526	(0.6408)	274	(191)	38	(53)	1	(4)
n19v	all	1.1132	(0.2505)	1.0038	(0.0053)	0.2386	(1.1492)	0.9962	(0.0010)	2.8911	(0.4083)	2085	(730)	262	(181)	3	(11)
n19v	water	0.8425	(0.2260)	0.9912	(0.0116)	2.5874	(2.3428)	0.9895	(0.0073)	3.1243	(0.6565)	1114	(510)	210	(167)	3	(11)
n19v	land	1.3741	(0.4148)	1.0030	(0.0087)	0.5958	(2.1593)	0.9917	(0.0031)	1.9293	(0.4683)	171	(215)	4	(15)	0	(0)
n19v	seaice	0.9035	(0.1875)	1.nsidc-0001	(0.0061)	0.8487	(1.3501)	0.9966	(0.0012)	2.2292	(0.2625)	231	(107)	15	(19)	0	(1)
n19v	si-exc	0.8304	(0.1681)	1.0018	(0.0057)	0.4061	(1.2678)	0.9987	(0.0006)	1.4899	(0.3168)	50	(60)	4	(11)	0	(0)
n22v	all	1.6364	(0.2570)	0.9999	(0.0067)	1.6366	(1.5170)	0.9928	(0.0023)	3.0968	(0.4433)	2635	(928)	354	(252)	4	(15)
n22v	water	1.4626	(0.2615)	0.9828	(0.0145)	5.1640	(3.1664)	0.9802	(0.0095)	3.7551	(0.7467)	1807	(742)	310	(236)	3	(14)
n22v	land	1.7972	(0.3873)	1.0024	(0.0091)	1.1974	(2.3359)	0.9918	(0.0030)	1.8707	(0.4522)	181	(255)	4	(15)	0	(0)
n22v	seaice	1.4970	(0.2291)	0.9984	(0.0084)	1.8421	(1.9240)	0.9943	(0.0027)	2.2768	(0.3656)	262	(162)	23	(33)	0	(0)
n22v	si-exc	1.4482	(0.2239)	1.0004	(0.0082)	1.3448	(1.8711)	0.9972	(0.0019)	1.6740	(0.4462)	87	(101)	9	(20)	0	(0)
n37h	all	-0.1377	(0.1986)	0.9978	(0.0055)	0.3035	(1.1636)	0.9897	(0.0035)	6.3582	(0.8595)	9246	(1783)	2724	(802)	233	(155)
n37h	water	-0.5007	(0.3622)	0.9647	(0.0271)	5.3757	(4.3467)	0.9605	(0.0213)	8.2104	(1.3946)	5738	(1226)	1989	(674)	212	(148)
n37h	land	0.2258	(0.2753)	0.9969	(0.0084)	0.9387	(2.0446)	0.9920	(0.0037)	2.7860	(0.8340)	709	(820)	87	(141)	1	(5)
n37h	seaice	-0.3681	(0.3056)	0.9975	(0.0087)	0.0477	(1.4693)	0.9909	(0.0047)	4.5787	(0.8250)	1161	(408)	246	(143)	12	(19)
n37h	si-exc	-0.3410	(0.2867)	1.0016	(0.0062)	-0.6778	(1.1515)	0.9954	(0.0030)	3.3684	(0.9576)	414	(274)	85	(95)	5	(12)
n37v	all	0.3078	(0.1680)	0.9875	(0.0074)	3.2019	(1.6511)	0.9888	(0.0038)	3.4015	(0.5002)	3063	(1140)	495	(276)	4	(12)
n37v	water	0.3532	(0.2307)	0.9468	(0.0345)	11.9432	(7.4746)	0.9543	(0.0277)	3.9058	(0.6801)	1823	(651)	371	(221)	3	(11)
n37v	land	0.2543	(0.2742)	0.9907	(0.0123)	2.6349	(3.2311)	0.9893	(0.0060)	2.5120	(0.8983)	560	(803)	67	(132)	1	(5)
n37v	seaice	0.2528	(0.2249)	0.9856	(0.0134)	3.5061	(2.9103)	0.9892	(0.0069)	2.2953	(0.4549)	243	(163)	23	(29)	0	(0)
n37v	si-exc	0.2266	(0.2169)	0.9895	(0.0115)	2.5802	(2.5019)	0.9941	(0.0050)	1.7267	(0.5195)	89	(103)	9	(18)	0	(0)
n91h	all	-0.0284	(0.2482)	0.9529	(0.0111)	10.6304	(2.1890)	0.9577	(0.0095)	7.7364	(0.5967)	62277	(6725)	16713	(3312)	730	(365)
n91h	water	0.0500	(0.3298)	0.8782	(0.0305)	26.1757	(6.2459)	0.8852	(0.0283)	9.5211	(1.0763)	38388	(5311)	11250	(3077)	502	(343)
n91h	land	-0.1211	(0.2965)	0.9689	(0.0160)	7.6224	(4.4897)	0.9744	(0.0133)	5.1839	(0.8079)	11105	(3791)	2107	(1131)	104	(135)
n91h	seaice	0.1024	(0.3826)	0.9444	(0.0208)	11.9142	(4.5370)	0.9497	(0.0159)	5.9602	(0.8159)	8101	(2837)	1830	(951)	74	(83)
n91h	si-exc	0.1659	(0.4054)	0.9562	(0.0212)	9.4275	(4.5323)	0.9613	(0.0173)	4.9919	(0.9997)	4063	(2066)	819	(644)	31	(48)
n91v	all	0.2637	(0.1816)	0.9707	(0.0146)	7.6232	(3.9830)	0.9737	(0.0103)	4.3668	(0.4724)	19304	(5438)	2798	(1282)	111	(144)
n91v	water	0.3234	(0.1742)	0.9511	(0.0301)	12.4816	(7.7724)	0.9551	(0.0238)	4.0374	(0.4233)	6962	(2055)	771	(381)	18	(32)
n91v	land	0.1999	(0.2760)	0.9689	(0.0218)	8.1636	(6.0746)	0.9727	(0.0174)	4.6348	(0.8894)	8728	(4078)	1598	(1061)	79	(111)
n91v	seaice	0.3435	(0.2624)	0.9722	(0.0253)	7.0782	(6.3947)	0.9765	(0.0167)	3.0092	(0.5578)	1822	(1191)	172	(190)	3	(8)
n91v	si-exc	0.3341	(0.2854)	0.9795	(0.0235)	5.2992	(5.8800)	0.9820	(0.0153)	2.5738	(0.6505)	838	(809)	73	(117)	1	(4)

Table 1: Means and standard deviations of daily values for the Northern Hemisphere in 2015.

Generally speaking, the F17 and F18 fields strongly correlate with each other. As expected, there is more difference between the two in the high frequency channels where stronger weather effects can be expected even over fairly short time scales such as the hour or so difference between the F17 and F18 passes.

		Bias		Slope		Intercept		Correlation		Std Dev		Num > 10K		Num > 20K		Num > 50K	
Chan	Mask	Mean	(StdDev)	Mean	(StdDev)	Mean	(StdDev)	Mean	(StdDev)	Mean	(StdDev)	Mean	(StdDv)	Mean	(StdDv)	Mean	(StdDv)
s19h	all	-0.0882	(0.3186)	1.0057	(0.0092)	-0.9407	(1.2372)	0.9945	(0.0044)	3.9977	(0.9692)	3340	(1384)	527	(523)	25	(203)
s19h	water	0.1642	(0.2845)	1.0020	(0.0124)	-0.5381	(1.5443)	0.9899	(0.0103)	4.4390	(0.9044)	3206	(1228)	507	(402)	20	(101)
s19h	land	0.1602	(0.5815)	1.0064	(0.0286)	-0.9358	(4.4766)	0.9983	(0.0103)	1.0872	(1.2295)	20	(237)	7	(124)	4	(81)
s19h	seaice	0.2504	(0.3790)	1.0075	(0.0067)	-1.0304	(0.9773)	0.9977	(0.0029)	3.1097	(0.8500)	557	(425)	44	(195)	4	(72)
s19h	si-exc	0.2499	(0.3912)	1.0082	(0.0066)	-1.1209	(0.9411)	0.9977	(0.0028)	3.1079	(0.8365)	529	(404)	42	(178)	3	(62)
s19v	all	0.7908	(0.2468)	0.9983	(0.0114)	1.1166	(2.2476)	0.9950	(0.0051)	2.1236	(0.6299)	638	(619)	70	(314)	6	(112)
s19v	water	0.8512	(0.2185)	0.9959	(0.0131)	1.6073	(2.5457)	0.9916	(0.0093)	2.3072	(0.5434)	600	(458)	62	(182)	2	(34)
s19v	land	0.5832	(0.4372)	1.0048	(0.0238)	-0.3998	(4.5475)	0.9985	(0.0078)	0.9233	(0.8719)	13	(166)	6	(105)	3	(63)
s19v	seaice	0.9592	(0.2458)	0.9997	(0.0088)	0.9904	(1.7878)	0.9978	(0.0036)	1.7182	(0.5808)	83	(230)	9	(127)	2	(36)
s19v	si-exc	0.9798	(0.2425)	1.0006	(0.0086)	0.8300	(1.7224)	0.9978	(0.0034)	1.6910	(0.5640)	76	(207)	8	(113)	2	(31)
s22v	all	1.1836	(0.2819)	0.9906	(0.0169)	3.1444	(3.4918)	0.9871	(0.0105)	2.8433	(0.7088)	1663	(976)	158	(366)	7	(124)
s22v	water	1.2919	(0.2570)	0.9831	(0.0210)	4.7717	(4.3123)	0.9806	(0.0173)	3.1459	(0.6409)	1615	(841)	148	(228)	2	(35)
s22v	land	0.8070	(0.5014)	1.0068	(0.0254)	-0.5766	(4.8251)	0.9985	(0.0087)	0.9332	(0.9623)	14	(202)	7	(123)	4	(73)
s22v	seaice	1.3030	(0.2642)	0.9955	(0.0130)	2.2518	(2.7801)	0.9952	(0.0062)	2.0250	(0.6492)	168	(285)	14	(144)	2	(40)
s22v	si-exc	1.3285	(0.2590)	0.9963	(0.0127)	2.0994	(2.6997)	0.9952	(0.0062)	2.0196	(0.6355)	159	(262)	13	(130)	2	(34)
s37h	all	-0.5028	(0.2860)	0.9814	(0.0182)	2.6220	(2.9656)	0.9764	(0.0147)	5.8395	(1.0456)	7846	(2348)	1637	(835)	67	(149)
s37h	water	-0.5903	(0.2702)	0.9650	(0.0405)	5.0105	(6.2967)	0.9599	(0.0371)	6.5730	(1.0951)	7666	(2217)	1606	(773)	63	(85)
s37h	land	-0.1598	(0.4889)	0.9947	(0.0245)	0.7808	(3.9516)	0.9983	(0.0090)	1.0520	(1.0123)	22	(215)	6	(97)	3	(61)
s37h	seaice	-0.4227	(0.3468)	0.9937	(0.0160)	0.6119	(2.6372)	0.9904	(0.0079)	4.2409	(0.8849)	1401	(655)	151	(216)	4	(48)
s37h	si-exc	-0.4209	(0.3463)	0.9934	(0.0167)	0.6476	(2.7188)	0.9898	(0.0089)	4.2968	(0.8704)	1350	(630)	145	(203)	3	(42)
s37v	all	0.0711	(0.2587)	0.9754	(0.0227)	5.3743	(4.8420)	0.9795	(0.0181)	2.7897	(0.6383)	1445	(912)	152	(273)	5	(82)
s37v	water	0.1611	(0.2432)	0.9441	(0.0506)	12.2138	(10.7992)	0.9540	(0.0479)	3.0784	(0.5936)	1371	(757)	139	(177)	2	(27)
s37v	land	-0.1999	(0.3944)	0.9985	(0.0199)	0.1071	(3.7004)	0.9985	(0.0068)	0.9517	(0.7823)	18	(177)	5	(85)	2	(45)
s37v	seaice	0.0254	(0.3116)	0.9747	(0.0261)	5.6231	(5.5652)	0.9846	(0.0196)	2.2346	(0.7505)	226	(328)	25	(113)	2	(29)
s37v	si-exc	0.0518	(0.3059)	0.9740	(0.0277)	5.7857	(5.9034)	0.9841	(0.0213)	2.2205	(0.7092)	201	(289)	21	(102)	2	(26)
s91h	all	-0.8141	(0.3898)	0.8994	(0.0284)	20.0382	(6.0677)	0.9061	(0.0270)	9.1283	(0.8901)	77099	(11297)	20888	(4661)	590	(538)
s91h	water	-0.8418	(0.4422)	0.8254	(0.0338)	36.1863	(7.2386)	0.8304	(0.0294)	10.3273	(0.9273)	75595	(10690)	20587	(4402)	573	(358)
s91h	land	-0.6518	(0.4445)	0.9840	(0.0240)	2.2932	(4.0683)	0.9951	(0.0103)	1.8160	(0.9968)	231	(849)	38	(546)	10	(182)
s91h	seaice	-0.8494	(0.4883)	0.9018	(0.0389)	19.9034	(8.1760)	0.9078	(0.0314)	7.2652	(0.9280)	18814	(6115)	3609	(1817)	56	(236)
s91h	si-exc	-0.8339	(0.5037)	0.8973	(0.0411)	20.8543	(8.6164)	0.9036	(0.0342)	7.4128	(0.9173)	18327	(6123)	3541	(1779)	54	(211)
s91v	all	-0.3670	(0.2784)	0.9852	(0.0117)	3.1284	(2.6535)	0.9820	(0.0094)	3.7505	(0.5656)	11192	(3669)	778	(1181)	24	(365)
s91v	water	-0.3126	(0.2810)	0.9127	(0.0364)	20.9641	(8.9350)	0.9093	(0.0275)	4.1203	(0.4753)	10547	(2945)	705	(680)	12	(146)
s91v	land	-0.5071	(0.3760)	0.9902	(0.0193)	1.4730	(3.5889)	0.9960	(0.0077)	1.6772	(0.8418)	207	(816)	31	(443)	9	(169)
s91v	seaice	-0.4460	(0.3311)	0.9590	(0.0377)	9.3656	(8.9670)	0.9524	(0.0263)	3.4556	(0.7304)	2880	(1922)	248	(616)	11	(171)
s91v	si-exc	-0.4281	(0.3374)	0.9552	(0.0379)	10.2899	(9.0422)	0.9496	(0.0264)	3.4577	(0.7056)	2696	(1831)	230	(567)	10	(145)

Table 2: Means and standard deviations of daily values for the Southern Hemisphere in 2015.

Summary of Conclusions

NSIDC compared gridded brightness temperatures from F17 and F18 for the period 01 January 2015 through 31 December 2015. Average TB biases between the sensors are less than 1°K except for the 22 GHz channel, which is sensitive to water vapor so larger differences are expected. Difference standard deviations are typically less than 5°K. Linear regression between the two sensors indicates slopes near 1 with y-intercepts near also near 1 except for larger values over water and for the 91 GHz, both of which are due to atmospheric emission; correlations are >0.95, with most >0.98.

The vast majority of observations are less than 10°K. Larger differences occur primarily either steep gradients in TBs across land-ocean or land-ice boundaries due to differences in sensor footprint patterns from the two sensors, or rapidly changing regions such as the sea ice edge or strong atmospheric from passing weather systems and differences in crossing times between the sensors. Smaller changes also result from slight calibration biases or effects of the daily composite gridding. Users should be aware of these differences as the product data source changes from F17 to F18.